Supplementary Figures 1-5

Metabolomic Analysis of Siderophore Cheater Mutants Reveals Metabolic Costs of Expression in Uropathogenic *Escherichia coli*

Haitao Lv[1, 2, 3]*, Chia S. Hung[1] and Jeffrey P. Henderson[1]*

[1]Center for Women's Infectious Diseases Research, Division of Infectious Diseases, Department of Medicine, Washington University School of Medicine, St. Louis, MO 63110, USA;

[2]Chongqing University Innovative Drug Research Center, Chongqing 401331, P. R. China;

[3]Tissue Repair and Regeneration Program, Institute of Health and Biomedical Innovation, Queensland University of Technology, Kelvin Grove, GLD 4059, Australia

Running title: Siderophore biosynthesis governing primary metabolism

* **Corresponding Authors**

Jeffrey P. Henderson, M.D., Ph.D., Phone: 01-314 454-8225. Fax: 01-314 454-5392.

E-mail: jhenderson@borcim.wustl.edu

Haitao Lv, Ph.D., Phone: 086-23-65678464. Fax: 086-23-65678450

E-mail: haitao.lu@cqu.edu.cn

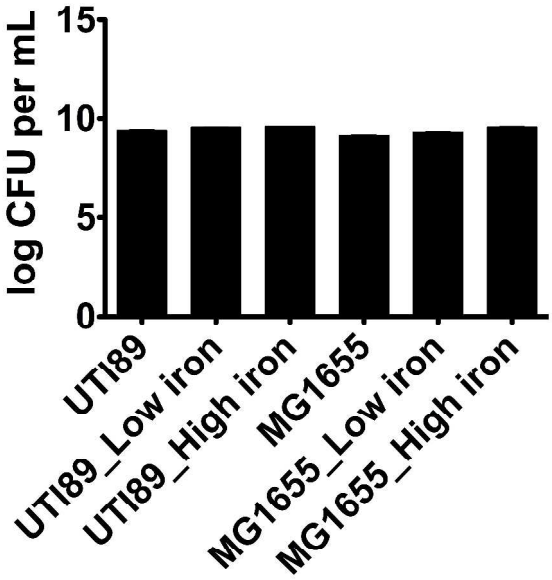

Supplementary Figure 1. Iron supplementation conditions modestly increase growth of both UTI89 and the non-pathogen MG1655. Growth was quantified by determining the number of colony forming units (CFU/mL) after 18 hours of growth.

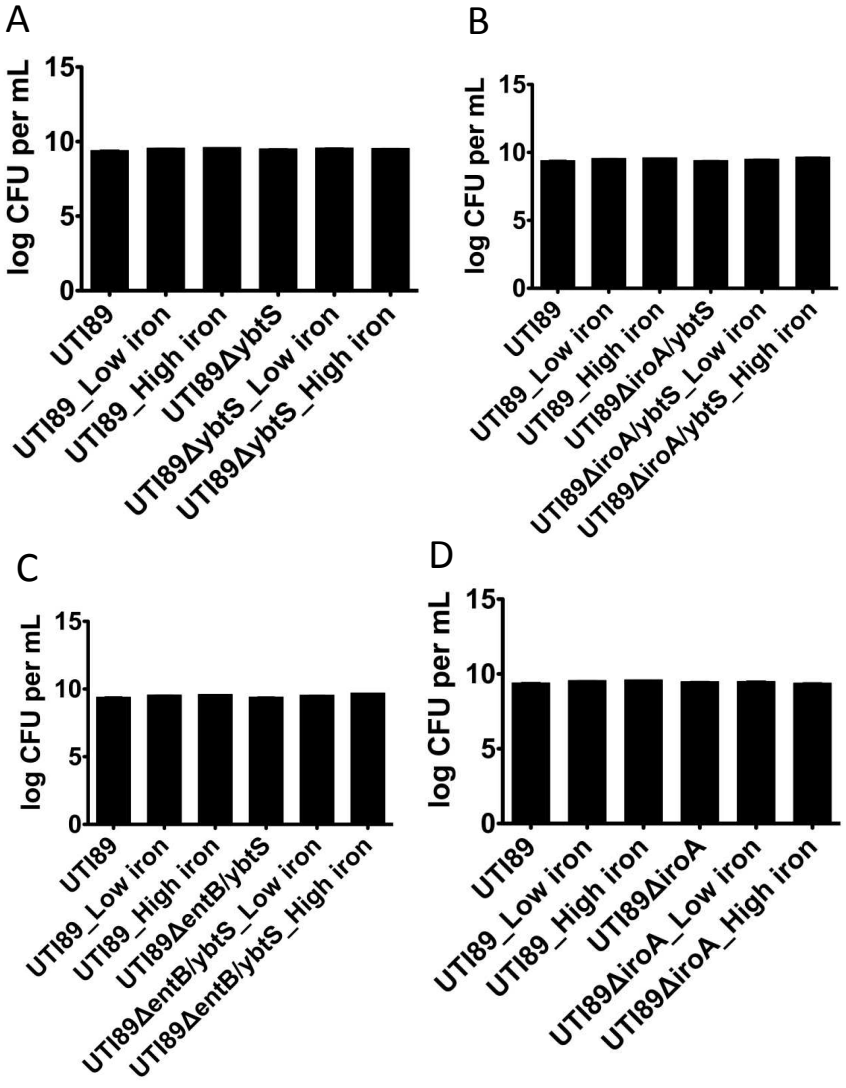

Supplementary Figure 2. UTI89 and its siderophore biosynthetic mutants exhibit similar growth. Colony forming units (CFU/mL) are shown with different levels of iron supplementation for wild type UTI89 and (A) UTI89Δ*entB/ybtS*, (B) UTI89Δ*iroA/ybtS,* (C) UTI89Δ*ybtS,* and (D) UTI89Δ*iroA* after 18 hours of growth.

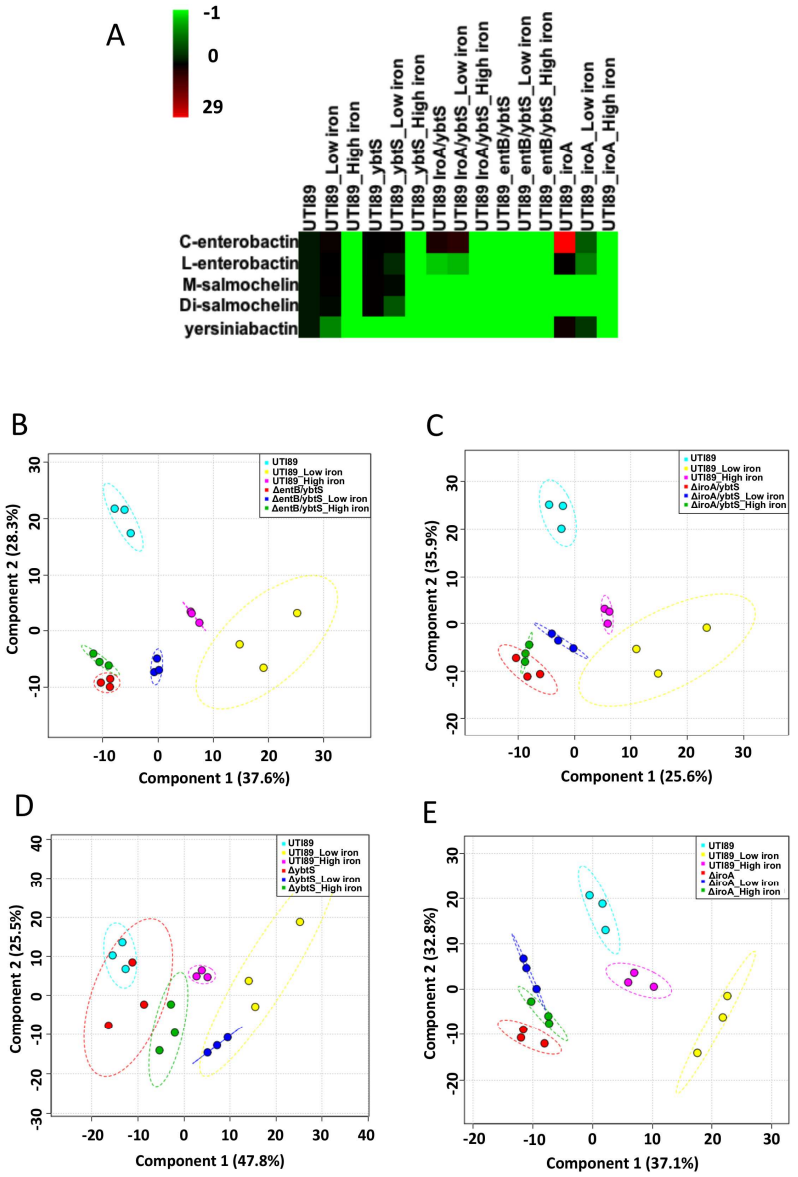

Supplementary Figure 3. Iron supplementation effects on siderophore biosynthesis and primary metabolism by UTI89 and its isogenic siderophore biosynthetic mutants. (A) Heat map depicting differences in siderophore expression by UTI89 and isogenic siderophore biosynthetic mutants with different iron supplementation levels. (B-E) PCA of primary metabolomes under different iron supplementation conditions for UTI89 compared to (B) UTI89Δ*entB/ybtS* lacking all siderophores, (C) UTI89Δ*iroA/ybtS* lacking salmochelin and yersiniabactin, (D) UTI89Δ*ybtS* lacking yersiniabactin, and (E) UTI89Δ*iroA* lacking salmochelin. UTI89Δ*ybtS* metabolomes are poorly distinguished from those of wild type UTI89 grown under the same condition while other mutants are well-distinguished from wild type. This overall pattern corresponds to conversion of enterobactin to salmochelin as a major contributor to *E.coli* primary metabolomic class.

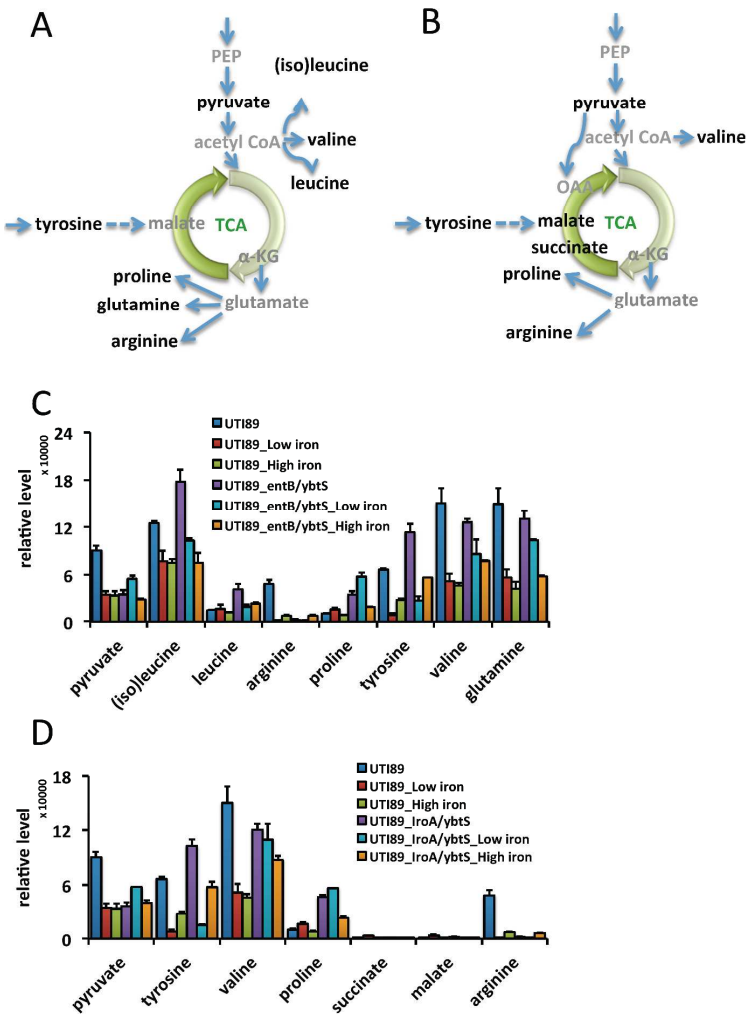

Supplementary Figure 4. Primary metabolites whose variations contribute most to between-strain differences. (A) Primary metabolites in UTI89 affected by iron supplementation and total siderophore deficiency (in black lettering) and their relationships to the TCA cycle, glycolysis and amino acid metabolism.
(B) Primary metabolites in UTI89 affected by iron supplementation and combined salmochelin-yersiniabactin deficiency (in black lettering) and their relationships to the TCA cycle, glycolysis and amino acid metabolism. (C,D) Primary metabolite levels for selected metabolites identified by VIP analysis differentiating UTI89 from (C) UTI89Δ*entB/ybtS* and (D) UTI89Δ*iroA/ybtS*.

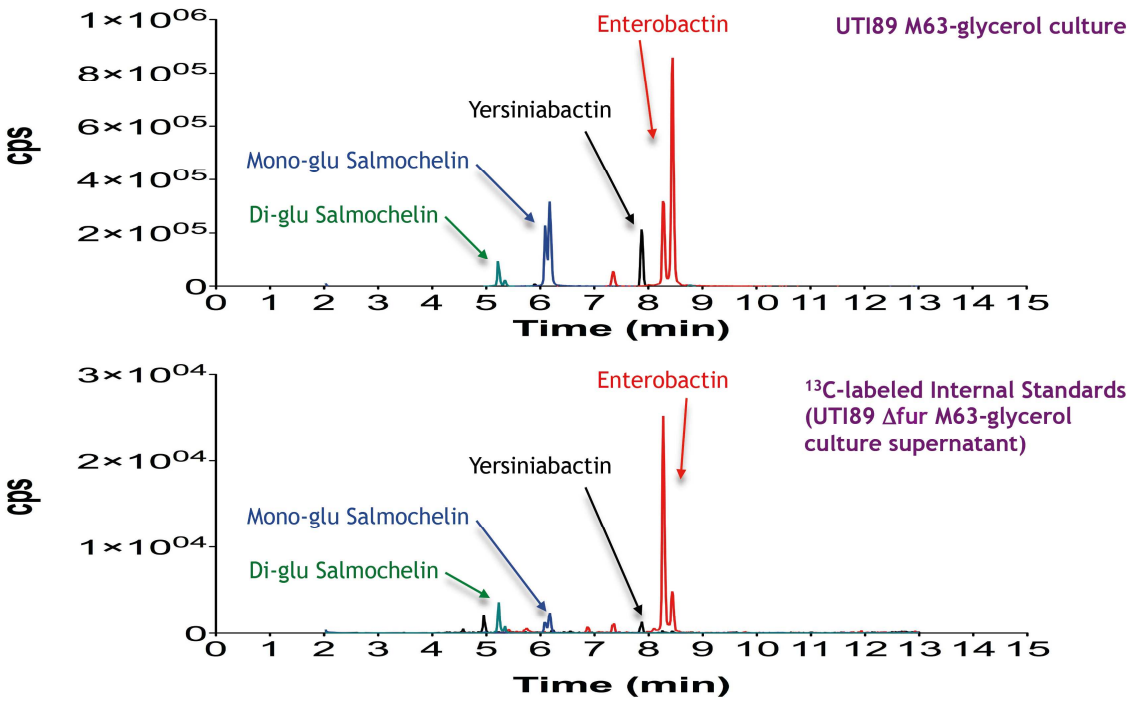

Supplementary Figure 5. LC-MS profile of ferric siderophores and 13C-labeled ferric siderophores (internal standard). Upper: Typical TIC plot of ferric siderophores; Lower: Typical TIC plot of $_{13}$C-labeled ferric siderophores (internal standard)